JOURNAL OF VIROLOGY, May 2002, p. 4855–4865 Vol. 76, No. 10
0022-538X/02/$04.00+0 DOI: 10.1128/JVI.76.10.4855–4865.2002
Copyright © 2002, American Society for Microbiology. All Rights Reserved.

Ebola Virus VP40 Drives the Formation of Virus-Like Filamentous Particles Along with GP

Takeshi Noda,[1,2] Hiroshi Sagara,[3] Emiko Suzuki,[3] Ayato Takada,[2] Hiroshi Kida,[1] and Yoshihiro Kawaoka[2,4]*

Laboratory of Microbiology, Department of Disease Control, Graduate School of Veterinary Medicine, Hokkaido University, Sapporo 060-0818,[1] and Division of Virology, Department of Microbiology and Immunology,[2] and Fine Morphology Laboratory, Department of Basic Medical Science,[3] Institute of Medical Science, University of Tokyo, Shirokanedai, Minato-ku, Tokyo 108-8639, Japan, and Department of Pathobiological Science, School of Veterinary Medicine, University of Wisconsin-Madison, Madison, Wisconsin 53706[4]

Received 13 November 2001/Accepted 12 February 2002

Using biochemical assays, it has been demonstrated that expression of Ebola virus VP40 alone in mammalian cells induced production of particles with a density similar to that of virions. To determine the morphological properties of these particles, cells expressing VP40 and the particles released from the cells were examined by electron microscopy. VP40 induced budding from the plasma membrane of filamentous particles, which differed in length but had uniform diameters of approximately 65 nm. When the Ebola virus glycoprotein (GP) responsible for receptor binding and membrane fusion was expressed in cells, we found pleomorphic particles budding from the plasma membrane. By contrast, when GP was coexpressed with VP40, GP was found on the filamentous particles induced by VP40. These results demonstrated the central role of VP40 in formation of the filamentous structure of Ebola virions and may suggest an interaction between VP40 and GP in morphogenesis.

Ebola virus, a member of the family *Filoviridae* in the order *Mononegavirales*, causes severe hemorrhagic fever in humans and nonhuman primates, resulting in high mortality rates (27). This enveloped, nonsegmented, negative-strand RNA virus (27) has a filamentous appearance, but its shape may be branched, circular, U- or 6-shaped, or long and straight (4). Virions have a uniform diameter of approximately 80 nm but vary greatly in length.

Ebola virus particles consist of seven structural proteins. The glycoprotein (GP) of Ebola virus forms spikes of approximately 7 nm, which are spaced at 5- to 10-nm intervals on the virion surface (4, 27). GP is the only transmembrane protein of Ebola virus and is responsible for receptor binding and membrane fusion (31). Cells infected with recombinant vaccinia virus expressing the GP produced virosomes that varied in shape and diameter but uniformly possessed spike structures on their surface (35), although the effects of more than 80 vaccinia virus proteins (23) on the formation of particles are unknown. Similar virosomes are also released from Ebola virus-infected cells (35). These findings suggest that the GP contributes not only to an early stage of the viral infection cycle but also to viral budding.

The Ebola virus VP40 protein, equivalent to the matrix protein of other negative-strand RNA viruses, is the most abundant protein in virions and is located beneath the viral membrane, where it presumably maintains the structural integrity of the particle (4). In enveloped viruses, matrix proteins play important roles in virus assembly and budding. In vesicular stomatitis virus (VSV), for example, the matrix protein drives the formation of vesicles (16, 19). The matrix protein of human parainfluenza virus type 1, expressed in mammalian cells, assembles into virus-like particles that are released into culture medium (2). The retroviral Gag protein assembles into particles that bud from the cell surface (3, 7, 10). These observations indicate that the matrix proteins of these enveloped viruses have an intrinsic ability to form virus-like particles.

The matrix proteins of many enveloped viruses are associated with the plasma membrane and are thought to interact with the cytoplasmic tails of viral glycoproteins. Such interaction is believed to be important for virus assembly. In influenza viruses, the removal of the cytoplasmic tail of the hemagglutinin or neuraminidase glycoprotein alters virion morphology (14, 22). Although not essential for normal particle formation in rabies virus and VSV, glycoproteins enhance the efficiency of particle formation (20, 21, 30). However, little is known about the VP40-GP interaction in Ebola virion formation.

Using biochemical assays, Jasenosky et al. (12) and others (11, 33) recently showed that expression of VP40 in mammalian cells leads to the production of particles with a density corresponding to that of virions in the culture medium. To determine the morphological properties of these particles and to understand the VP40-GP interaction during virion morphogenesis, we used electron microscopy to examine cells expressing VP40 or GP alone or those expressing both proteins.

MATERIALS AND METHODS

Cells. 293T human embryonic kidney cells were maintained in Dulbecco's modified Eagle medium supplemented with 10% fetal calf serum, L-glutamine and penicillin-streptomycin-gentamicin solution (24). The cells were grown in an incubator at 37°C under 5% CO_2.

Plasmids. Full-length cDNAs encoding the Ebola virus (species Zaire) VP40 or GP were cloned separately into a mammalian expression vector, pCAGGS/

* Corresponding author. Mailing address: Institute of Medical Science, University of Tokyo, Shirokanedai, Minato-ku, Tokyo 108-8639, Japan. Phone: 81-3-5449-5310. Fax: 81-3-5449-5408. E-mail: kawaoka@ims.u-tokyo.ac.jp

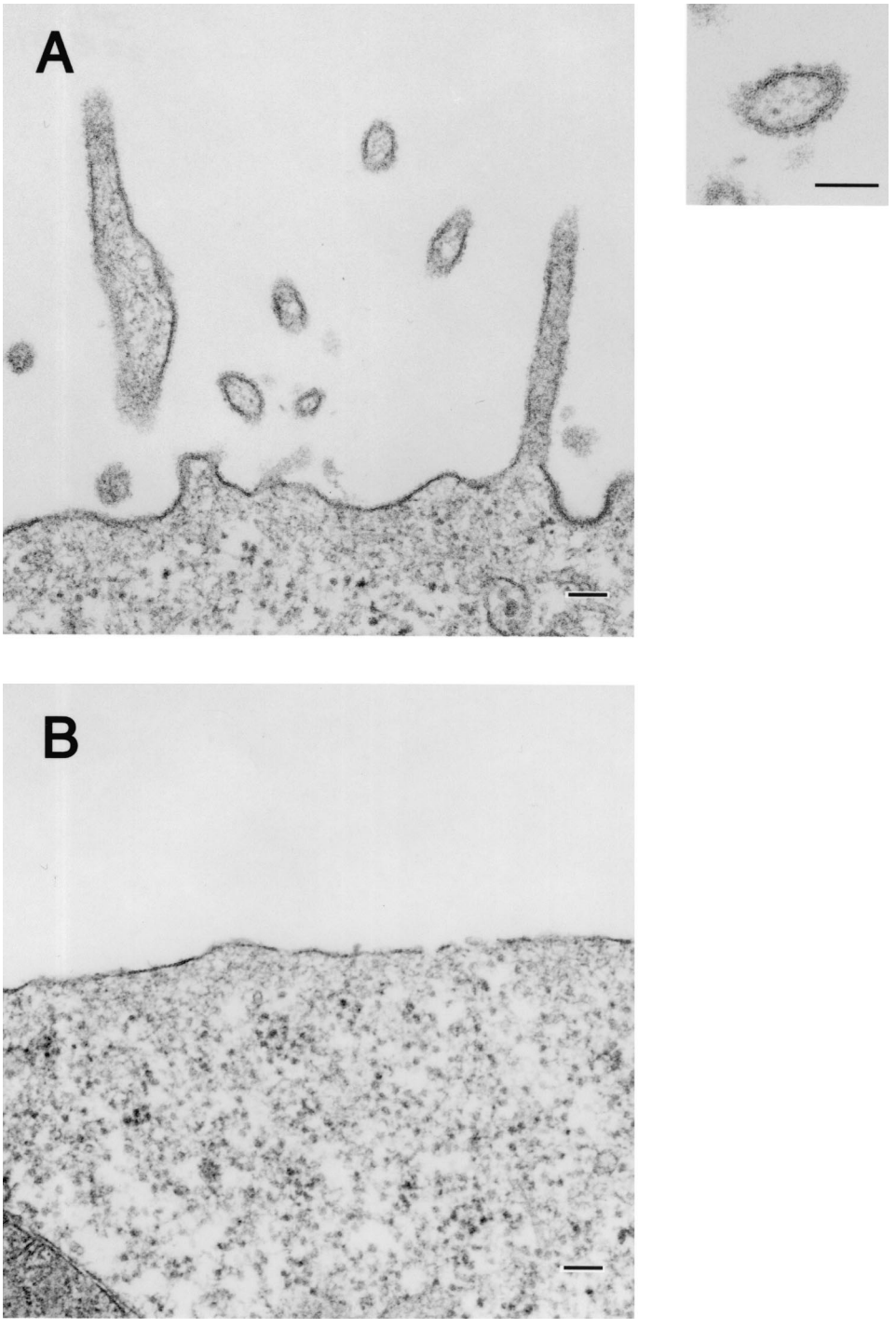

FIG. 1. Budding of GP-associated particles from the plasma membrane. (A) 293T cells at 24 h posttransfection with a GP-expressing plasmid. (B) 293T cells transfected with an empty expression vector lack such particle formation. Bars, 100 nm.

MCS (17, 25), which contains the chicken β-actin promoter. The resulting constructs were designated pCEboZVP40 and pCEboZGP, respectively.

Cell transfection for expression of VP40 and GP. 293T cells (10^6) were transfected with plasmids using the Trans IT LT-1 reagent (Panvera, Madison, Wis.) according to the manufacturer's instructions. Briefly, 1 μg of DNA in 0.1 ml of Opti-MEM (Gibco-BRL) and 3 μl of the transfection reagent were mixed, incubated for 10 min at room temperature, and added to the cells. Transfected cells were incubated at 37°C for 24 or 48 h.

Electron microscopy. Ultrathin-section electron microscopy was performed as follows. Twenty-four hours posttransfection of 293T cells with plasmids, the cells were washed with phosphate-buffered saline (PBS) and fixed for 20 min with 2.5% glutaraldehyde (GLA) in 0.1 M cacodylate buffer (pH 7.4). They were scraped off the dish, pelleted by low-speed centrifugation, and then fixed for 30 min with the same fixative. Small pieces of fixed pellet were washed with the same buffer, postfixed with 2% osmium tetroxide in the same buffer for 1 h at 4°C, dehydrated with a series of ethanol gradients followed by propylene oxide, embedded in Epon 812 Resin mixture (TAAB), and polymerized at 70°C for 2 days. For immunoelectron microscopy, cells were fixed with 4% paraformaldehyde and 0.1% GLA, dehydrated, and embedded in LR White Resin (London Resin Company Ltd.). Thin sections were stained with uranyl acetate and lead

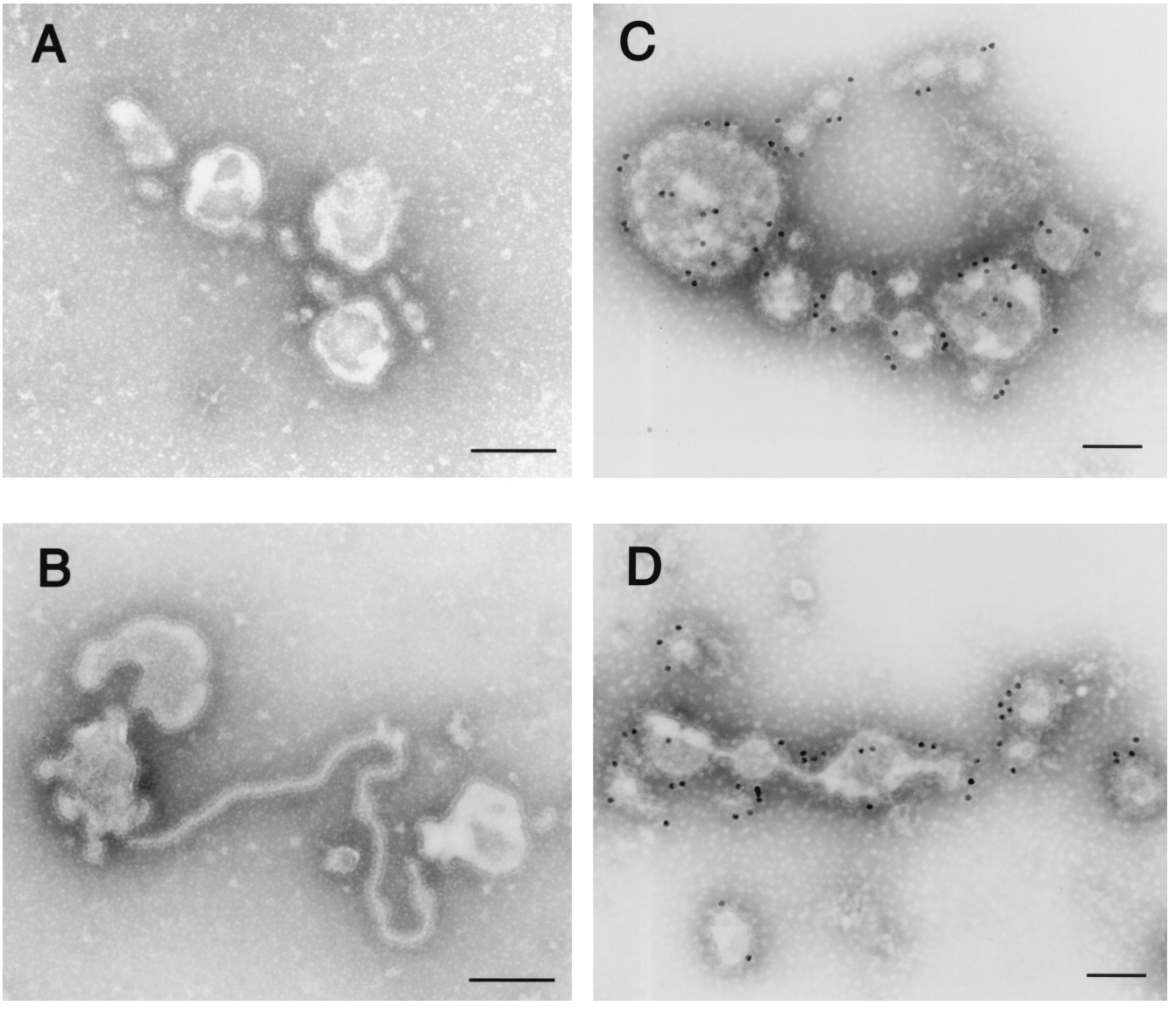

FIG. 2. Pleomorphic particles resulting from GP expression. The supernatants of cells expressing GP were centrifuged through 20% sucrose, and the pelleted material was then negatively stained with 2% PTA. (A and B) Pleomorphic particles with surface spikes were observed. (C and D) Pelleted material was immunolabeled with a mixture of anti-GP monoclonal antibodies conjugated to 15-nm gold particles. Bars, 100 nm.

citrate and examined with a JEM-1200EX electron microscope at 80 kV. For negative staining, culture media of 293T cells were collected at 24 h posttransfection onto a Formvar-coated copper grid, stained with 2% phosphotungstic acid solution (PTA), and examined with a JEM-1200 electron microscope at 80 kV. For immunoelectron microscopy, the samples were adsorbed to Formvar-coated nickel grids and washed with PBS containing 0.5% bovine serum albumin (PBS-BSA). The grids were then treated with mouse anti-GP monoclonal antibody (a mixture of ZGP12, ZGP42, and ZGP133 [32]; 1:150 in PBS-BSA) or rabbit anti-VP40 polyclonal antibody (1:300 in PBS-BSA) and rinsed six times with PBS, followed by incubation with a goat antimouse immunoglobulin conjugated to 15-nm gold particles (1:50 dilution; BB International) or a goat antirabbit immunoglobulin conjugated to 5-nm gold particles (1:100 dilution; BB International). After washing, the samples were fixed for 10 min in 2% glutaraldehyde and negatively stained with 2% PTA.

RESULTS

Pleomorphic particle formation by GP. To determine the morphology of vesicles induced by Ebola virus GP expression, we analyzed GP-expressing cells and their supernatants by electron microscopy. The ultrathin sections of these cells showed particle-like structures with surface spikes budding from the plasma membrane (Fig. 1A); no such structures were observed using cells transfected with the expression vector alone (Fig. 1B). The spikes, which extended approximately 10 nm from the lipid membrane of the particle-like structure, did not seem to have a particularly ordered arrangement (Fig. 1A, inset). As previously observed with the recombinant vaccinia virus system (35), pleomorphic structures similar to virosomes with a range of diameters were apparent in the supernatants of GP-expressing cells (Fig. 2A and B). The spikes on the surface of the vesicles reacted with a mixture of anti-GP monoclonal antibodies (Fig. 2C and D), confirming the GP derivation of the structures.

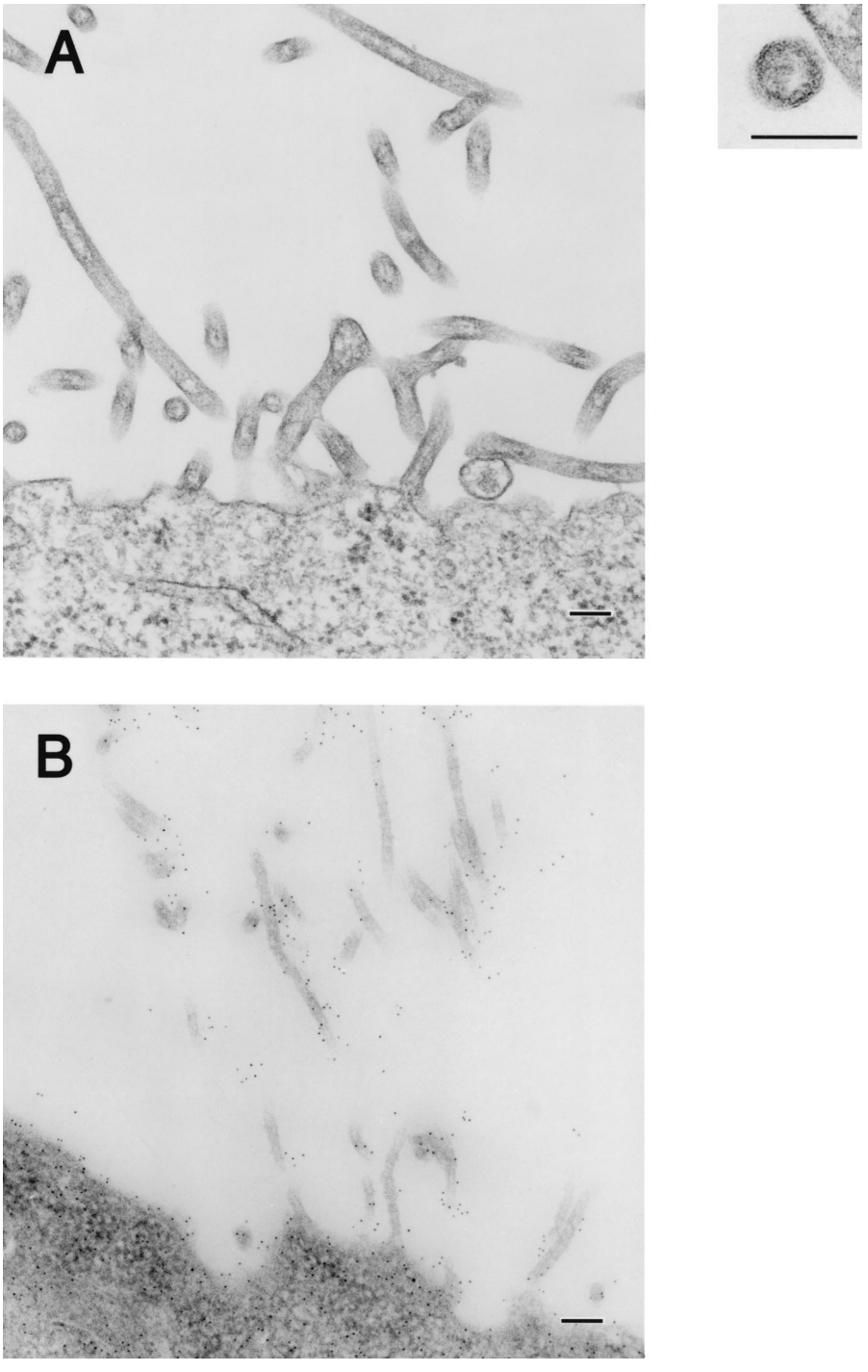

FIG. 3. Morphological changes in 293T cells expressing VP40. At 24 h posttransfection of 293T cells with a VP40-expressing plasmid, filamentous particles budding from the plasma membrane (A), membrane ruffles and the adhering site of two bilayers (C, arrows), as well as aggregated ribosomes (E, arrows) were apparent. Intracellular electron-dense filamentous structures (F, arrowheads) were also observed. (B and D) The filamentous particles and membrane ruffles were immunolabeled with an anti-VP40 antibody conjugated with 5-nm gold particles. M, mitochondrion; mt, microtubule. Bars, 100 nm (panels A, B, C, D, and F) or 200 nm (panel E).

VP40 induces filamentous particle formation. To determine how VP40 protein expressed in 293T cells is released into culture medium (11, 12, 33), we analyzed the VP40-expressing cells by transmission electron microscopy. The ultrathin sections of the cells expressing VP40 showed budding of filamentous structures (approximately 65 nm in diameter) on the cell surface (Fig. 3A). In some cells, the plasma membranes appeared ruffled and to consist of two bilayers (Fig. 3C). Aggregated ribosomes (Fig. 3E, arrows) were occasionally found in the cytoplasm of cells expressing VP40, as were electron-dense

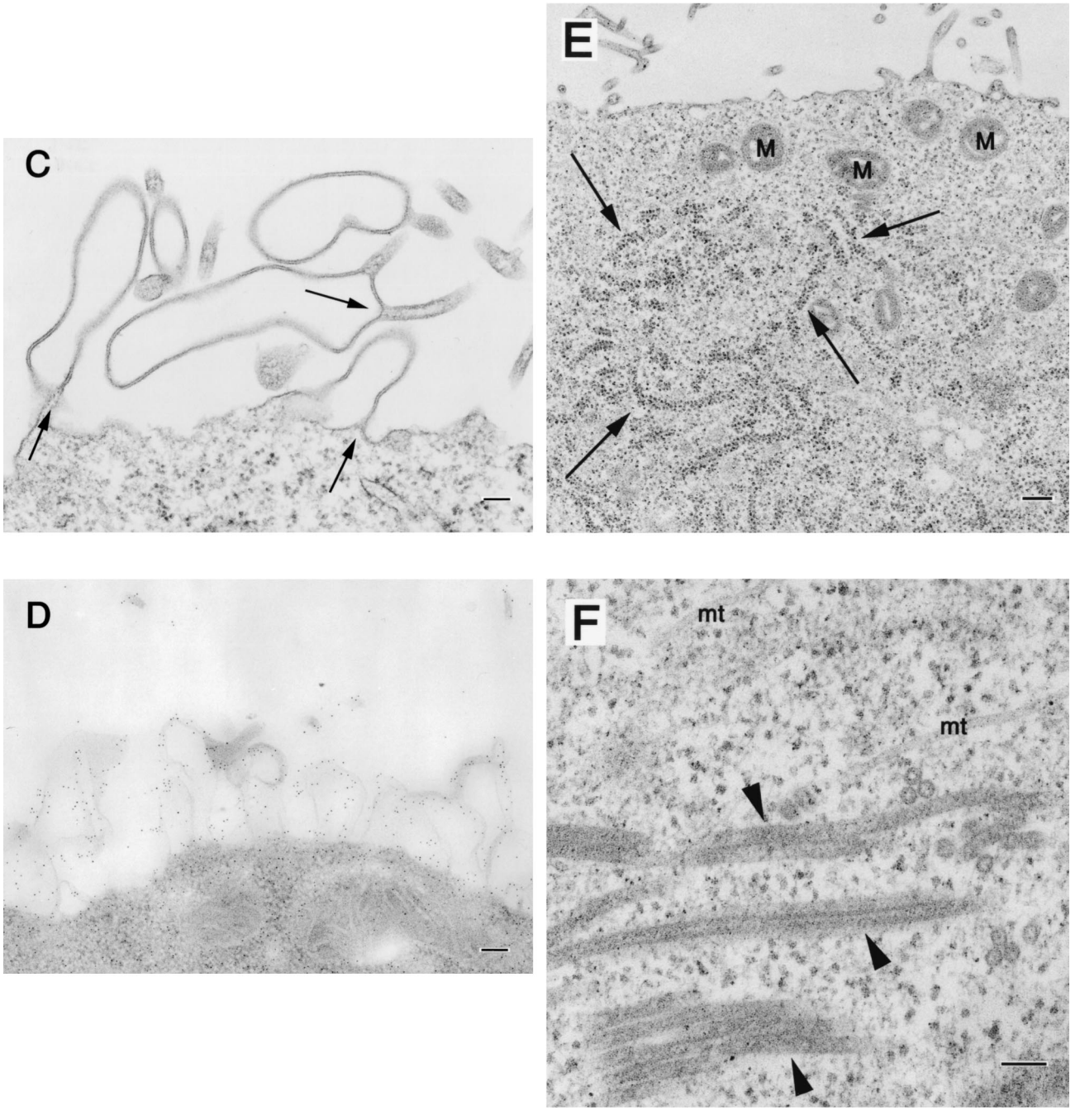

FIG. 3—*Continued*.

filamentous structures (approximately 45 nm in diameter; Fig. 3F, arrowheads), which were never seen in cells transfected with the expression vector alone. The budding particles and membrane ruffles reacted with rabbit anti-VP40 polyclonal antibody (Fig. 3B and D), confirming that VP40 had contributed to the generation of these structures. In studies to further determine the size and morphology of the VP40 particles released from cells, the supernatants of cells expressing this protein were centrifuged through 20% sucrose and the pelleted material was negatively stained with 2% PTA and analyzed by electron microscopy. Filamentous particles, which had uniform diameters of approximately 65 nm but varied lengths, were observed (Fig. 4A through C). These results indicate that VP40 alone can induce the formation of filamentous particles which bud from the cell surface.

VP40-GP interaction in particle morphogenesis. To determine how GP expression affects VP40-driven particle formation, we transfected 293T cells with both VP40- and GP-expressing plasmids. In ultrathin sections of the tranfected cells, we observed filamentous particle-like structures of 80-nm external diameter that were budding from the plasma membrane (Fig. 5).

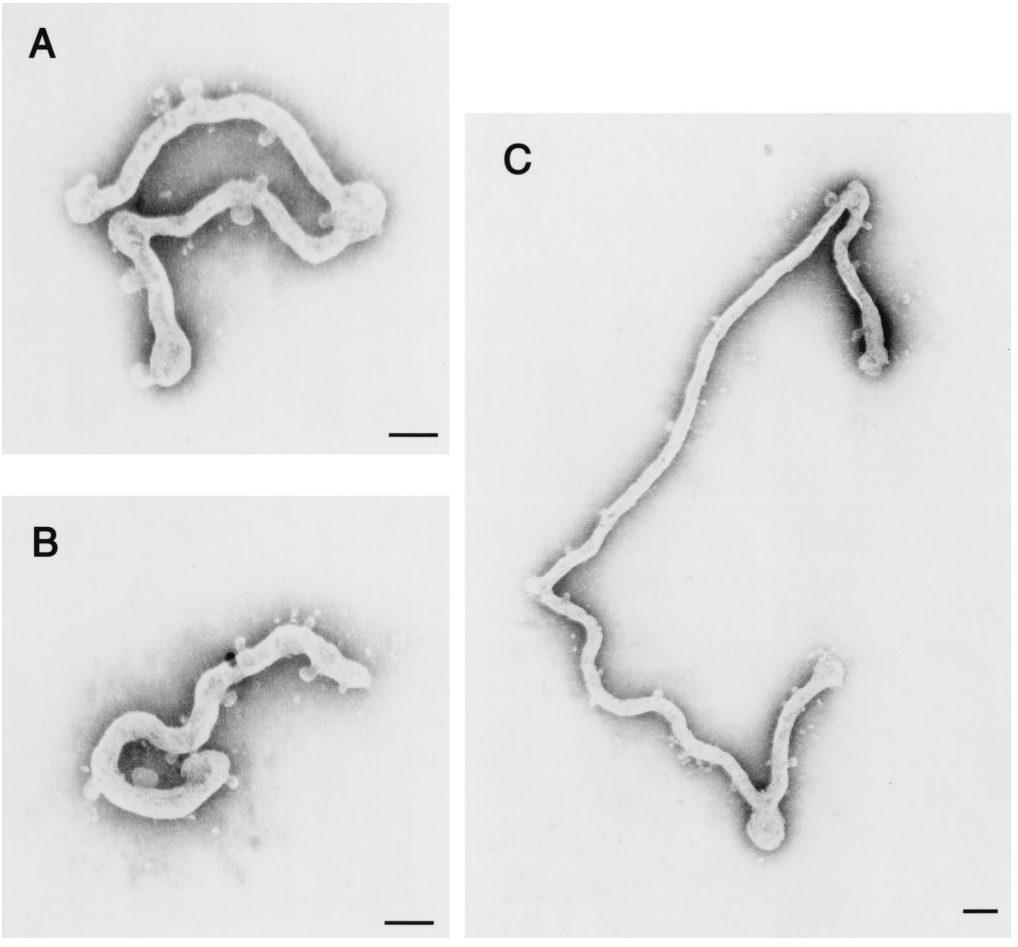

FIG. 4. Filamentous particles induced by VP40 expression. The supernatants of cells expressing VP40 were centrifuged through 20% sucrose, and the pelleted material was then negatively stained with 2% PTA. Particles with uniform diameters of approximately 65 nm and varied lengths were observed. Bars, 100 nm.

The structures possessed spikes of approximately 10 nm on their surface, in contrast to the structures observed in cells expressing VP40 alone (Fig. 3A). Also, in contrast to the arrangement of the spikes on the pleomorphic structures induced by GP expression, the spikes on the filamentous particles seemed to have an ordered arrangement (Fig. 5A, inset). Also, unlike the findings for expression of GP alone, few pleomorphic particles were observed. The particle structures were studied in more detail after negative staining of the particles in culture supernatants of cells expressing both VP40 and GP. Filamentous Ebola virus-like particles with surface spikes of approximately 85-nm in external diameter and lengths that ranged to 10 μm were observed (Fig. 6A through C). The spikes projected from the particle surface at 5- to 10-nm intervals and were morphologically indistinguishable from those on the Ebola virion surface (4, 27). Labeling the spikes with a mixture of anti-GP monoclonal antibodies conjugated with gold particles confirmed their identity as GP (Fig. 6D). Furthermore, when treated with 0.03% Triton X-100 and with both the anti-VP40 antibody conjugated to 5-nm gold particles and a mixture of anti-GP monoclonal antibodies conjugated to 15-nm gold particles, the filamentous particles became labeled with both antibodies, demonstrating that the Ebola virus-like particles contained GP as well as VP40 proteins (Fig. 6E). These results demonstrate GP incorporation into VP40-generated filamentous structures without affecting filamentous particle formation.

DISCUSSION

A hallmark of Ebola viruses is their filamentous virions, as suggested by the family name *Filoviridae*. The shapes of enveloped viruses are determined by viral proteins of retroviruses (1, 5, 15) or by both viral RNA length and proteins of VSV (26). Because specific interactions among viral components are required for the formation of defined virion shapes, an understanding of such interactions can lead to the identification of targets for the development of antiviral compounds.

Here we showed by electron microscopy that the expression of VP40 in the absence of any other Ebola virus proteins leads to the formation of filamentous particles which resemble spikeless virions released into the supernatant of cultured Ebola virus-infected cells (6). Thus, our results suggest that the Ebola virus VP40 possesses structural information necessary and sufficient to induce the formation of filamentous particles, which then bud from the plasma membrane. Interestingly, some fil-

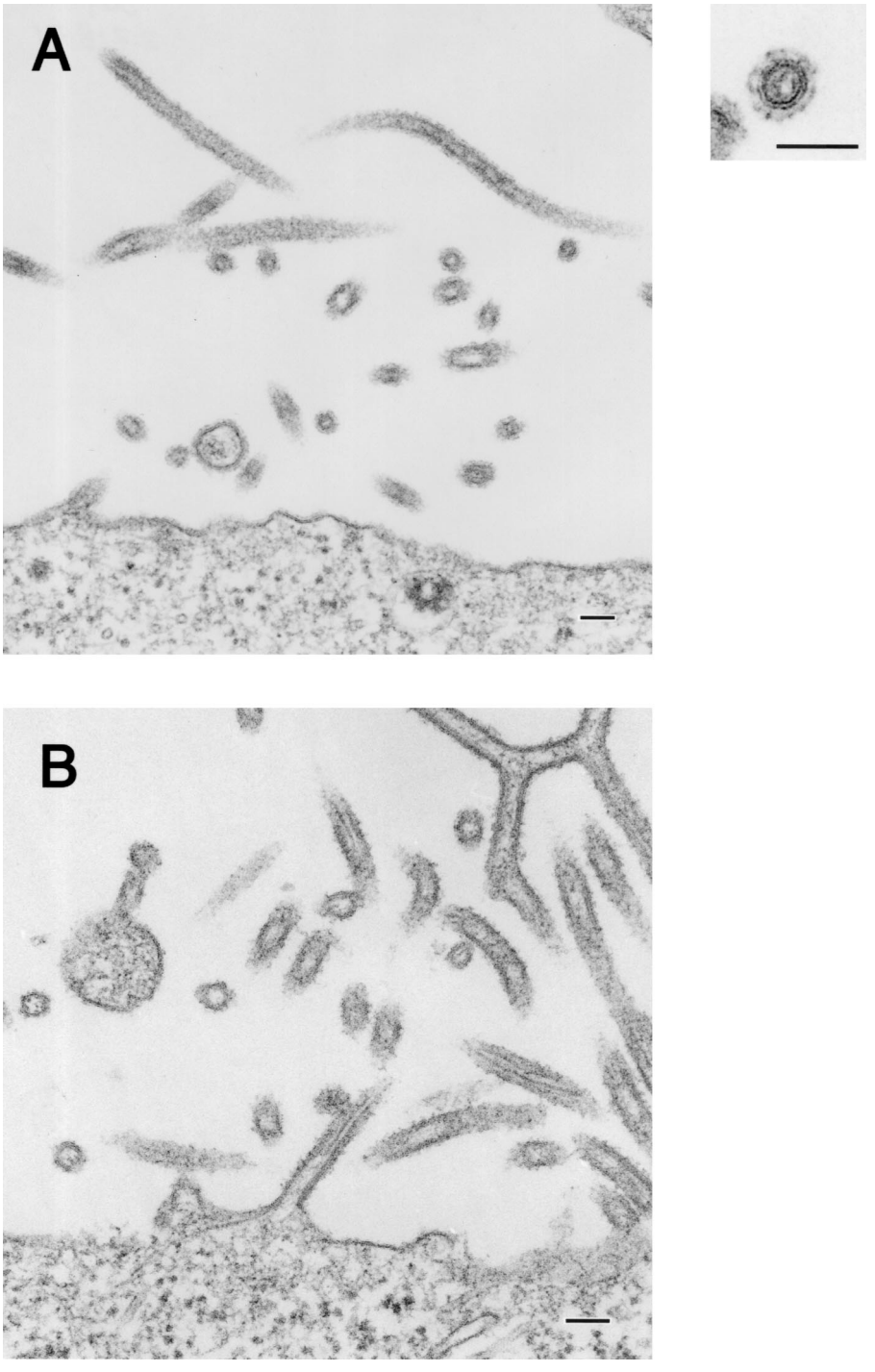

FIG. 5. Filamentous, spiked particles budding from the plasma membrane at 24 h posttransfection of 293T cells with plasmids coexpressing VP40 and GP. Bars, 100 nm.

amentous structures were observed in the cytoplasm of cells expressing VP40 as have been found in the cytoplasm of the cells infected with Ebola virus. Similar structures have also been observed in cells expressing the M1 protein of influenza virus or the Gag protein of retroviruses (3, 7, 9). However, the tubular structures observed upon expression of influenza virus M1 alone were not seen during normal viral infection or when M1 was coexpressed with other influenza virus proteins. Thus, VP40 may form intracellular filamentous structures by self-aggregation.

Membrane ruffles containing VP40 protein were observed in some VP40-expressing cells (Fig. 3C and D). The M protein of VSV induces similar double-layered membranes at the cell surface when expressed from recombinant Sendai virus (29). IpaC protein secreted by *Shigella flexneri* has also been linked to large-

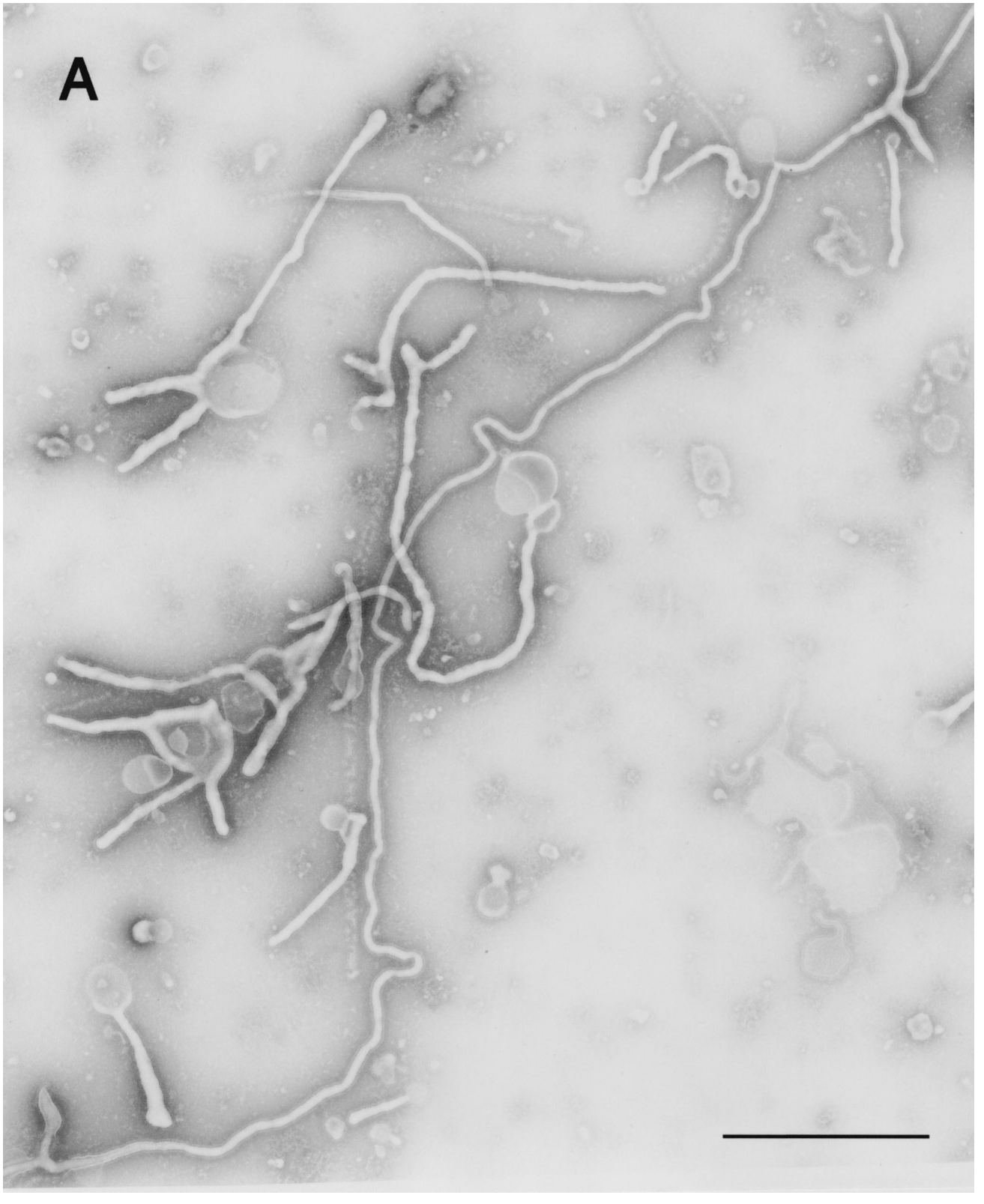

FIG. 6. Ebola virus-like particles produced by coexpression of VP40 and GP. The supernatants of cells coexpressing these two proteins were centrifuged through 20% sucrose, and the pelleted material was then negatively stained with 2% PTA. (A through C) Filamentous particles with surface spikes and varied lengths were observed. Pelleted material was immunolabeled with a mixture of anti-GP monoclonal antibodies conjugated to 15-nm gold particles (D, arrowheads), treated with 0.03% Triton X-100 at room temperature for 15 min, and then immunolabeled with a mixture of anti-GP antibodies conjugated to 15-nm gold particles (E, arrowheads) and an anti-VP40 antibody conjugated to 5-nm gold particles (E, arrows). Bars, 1 μm (panel A) or 100 nm (panels B through E).

FIG. 6—*Continued*.

scale membrane extension in macrophages, including lamellipodia and membrane ruffles (18, 34), while *Salmonella enterica* serovar Typhimurium triggers the formation of host cell membrane ruffles in nonphagocytic cells (8, 36). These membrane ruffles are thought to result from interactions between the bacterial proteins, including IpaC, and the actin cytoskeletons of host cells (34, 36). In Ebola virus-infected cells, host cell plasma membranes proliferate extensively at the peak stage of viral budding (6), as observed in cells expressing VP40 alone. Thus, VP40 may interact with actin filaments during the assembly or budding of Ebola virus at the cell surface.

The impact of glycoprotein interaction with the matrix protein on virion morphology differs among viruses. For example, deletion of the cytoplasmic tails of the influenza virus hemagglutinin and neuraminidase alters virus morphology (14, 22), while the characteristic morphologies of rabies virus and VSV do not depend on glycoprotein-matrix protein interaction (20, 21, 28, 30). The Ebola virus GP, like that of VSV G, was incorporated into filamentous particles without affecting the morphology of the particles. However, such interaction may contribute to the efficiency of budding, as demonstrated by research with VSV (13, 21).

In conclusion, we demonstrated that VP40 induces VP40 containing-filamentous particle formation and that GP spikes are incorporated into VP40 induced-filamentous particles upon coexpression of GP and VP40, resulting in Ebola virus-like particles. This virus-like particle formation system will be useful to further elucidate the mechanism of Ebola virus particle formation, including the functional link between Ebola virus and cellular components.

ACKNOWLEDGMENTS

We thank Krisna Wells and Martha McGregor for excellent technical assistance and John Gilbert for editing the manuscript.

This work was supported by Grants-in-Aid from the Ministry of Education, Culture, Sports, Science and Technology and the Ministry of Health, Labor and Welfare, Japan, and by a grant from the National Institute of Allergy and Infectious Diseases (NIH).

REFERENCES

1. **Campbell, S., and V. M. Vogt.** 1997. In vitro assembly of virus-like particles with Rous sarcoma virus Gag deletion mutants: identification of the p10 domain as a morphological determinant in the formation of spherical particles. J. Virol. **71:**4425–4435.
2. **Coronel, E. C., K. G. Murti, T. Takimoto, and A. Portner.** 1999. Human parainfluenza virus type 1 matrix and nucleoprotein genes transiently expressed in mammalian cells induce the release of virus-like particles containing nucleocapsid-like structures. J. Virol. **73:**7035–7038.
3. **Delchambre, M., D. Gheysen, D. Thines, C. Thiriart, E. Jacobs, E. Verdin, M. Horth, A. Burny, and F. Bex.** 1989. The Gag precursor of simian immunodeficiency virus assembles into virus-like particles. EMBO J. **8:**2653–2660.
4. **Feldmann, H., and H. D. Klenk.** 1996. Marburg and Ebola viruses. Adv. Virus Res. **47:**1–52.
5. **Gay, B., J. Tournier, N. Chazal, C. Carriere, and P. Boulanger.** 1998. Morphopoietic determinants of HIV-1 Gag particles assembled in baculovirus-infected cells. Virology **247:**160–169.
6. **Geisbert, T. W., and P. B. Jahrling.** 1995. Differentiation of filoviruses by electron microscopy. Virus Res. **39:**129–150.
7. **Gheysen, D., E. Jacobs, F. de Foresta, C. Thiriart, M. Francotte, D. Thines, and M. De Wilde.** 1989. Assembly and release of HIV-1 precursor Pr55^{gag} virus-like particles from recombinant baculovirus-infected insect cells. Cell **59:**103–112.
8. **Ginocchio, C. C., S. B. Olmsted, C. L. Wells, and J. E. Galan.** 1994. Contact with epithelial cells induces the formation of surface appendages on Salmonella typhimurium. Cell **76:**717–724.
9. **Gomez-Puertas, P., C. Albo, E. Perez-Pastrana, A. Vivo, and A. Portela.** 2000. Influenza virus matrix protein is the major driving force in virus budding. J. Virol. **74:**11538–11547.
10. **Haffer, O., J. Garrigues, B. Travis, P. Moran, J. Zarling, and S. L. Hu.** 1990. Human immunodeficiency virus-like, nonreplicating, *gag-env* expression system. J. Virol. **64:**2653–2659.
11. **Harty, R. N., M. E. Brown, G. Wang, J. Huibregtse, and F. P Hayes.** 2000. A PPxY motif within the VP40 protein of Ebola virus interacts physically and functionally with a ubiquitin ligase: implications for filovirus budding. Proc. Natl. Acad. Sci. USA **97:**13871–13876.
12. **Jasenosky, L. D., G. Neumann, I. Lukashevich, and Y. Kawaoka.** 2001. Ebola virus VP40-induced particle formation and association with the lipid bilayer. J. Virol. **75:**5205–5214.
13. **Jayakar, H. R., K. G. Murti, and M. A. Whitt.** 2000. Mutations in the PPPY motif of vesicular stomatitis virus matrix protein reduce virus budding by inhibiting a late step in virion release. J. Virol. **74:**9818–9827.
14. **Jin, H., G. P. Leser, J. Zhang, and R. A. Lamb.** 1997. Influenza virus hemagglutinin and neuraminidase cytoplasmic tails control particle shape. EMBO J. **16:**1236–1247.
15. **Joshi, S. M., and V. M. Vogt.** 2000. Role of the Rous sarcoma virus p10 domain in shape determination of *gag* virus-like particles assembled in vitro and within *Escherichia coli*. J. Virol. **74:**10260–10268.
16. **Justice, P. A., W. Sun, Y. Li, Z. Ye, P. R. Grigera, and R. P. Wagner.** 1995.

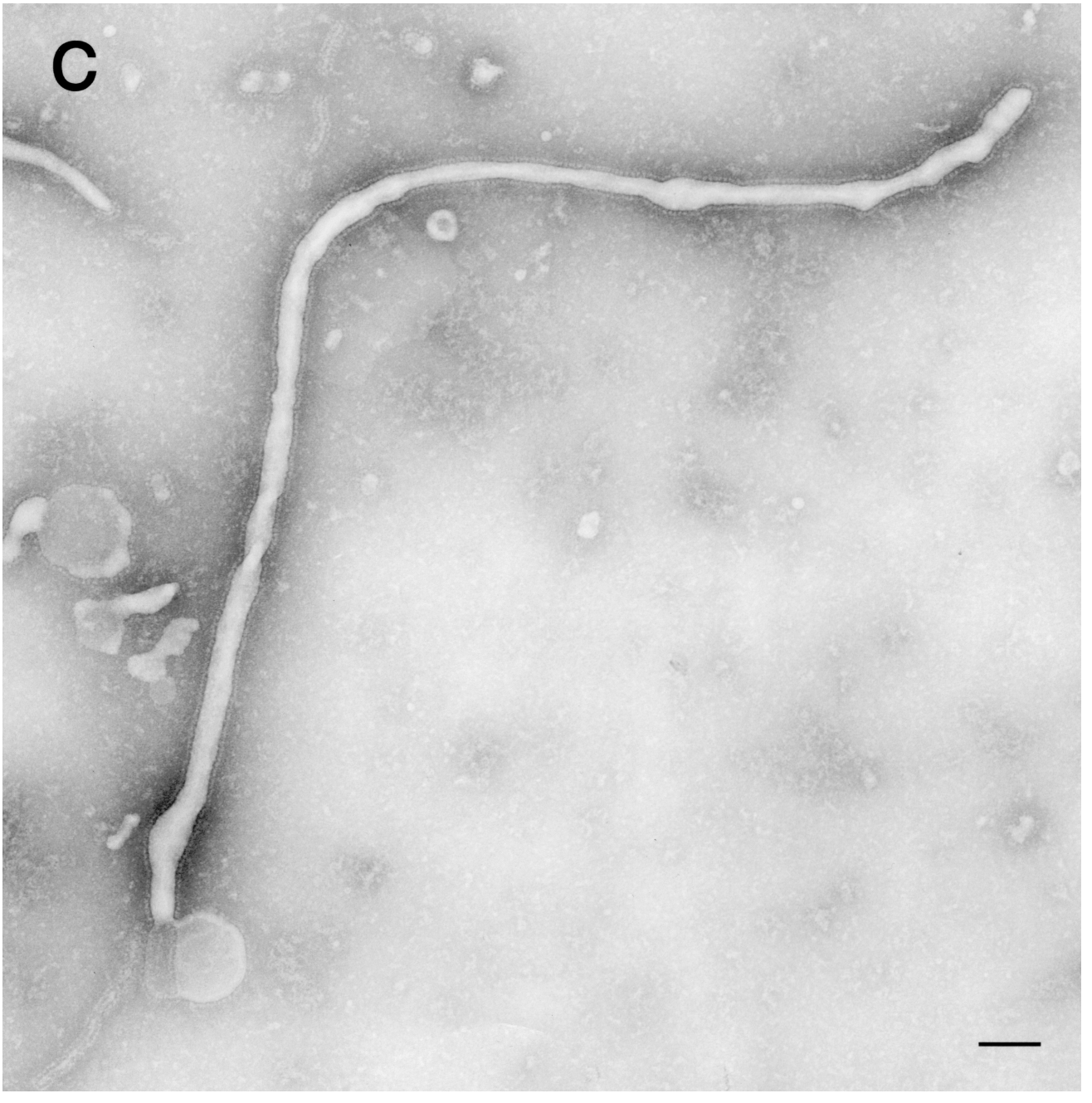

FIG. 6—*Continued*.

Membrane vesiculation function and exocytosis of wild-type and mutant matrix proteins of vesicular stomatitis virus. J. Virol. **69:**3156–3160.

17. **Kobasa, D., M. E. Rodgers, K. Wells, and Y. Kawaoka.** 1997. Neuraminidase hemadsorption activity, conserved in avian influenza A viruses, does not influence viral replication in ducks. J. Virol. **71:**6706–6713.
18. **Kuwae, A., S. Yoshida, K. Tamano, H. Mimuro, T. Suzuki, and C. Sasakawa.** 2001. *Shigella* invasion of macrophage requires the insertion of IpaC into host plasma membrane. J. Biol. Chem. **276:**32230–32239.
19. **Li, Y., L. Luo, M. Schubert, R. P. Wagner, and C. Y. Kang.** 1993. Viral liposomes released from insect cells infected with recombinant baculovirus expressing the matrix protein of vesicular stomatitis virus. J. Virol. **67:**4415–4420.
20. **Mebatsion, T., M. Konig, and K. K. Conzelmann.** 1996. Budding of rabies virus particles in the absence of the spike glycoprotein. Cell **84:**941–951.
21. **Mebatsion, T., F. Weiland, and K. K. Conzelmann.** 1999. Matrix protein of rabies virus is responsible for the assembly and budding of bullet-shaped particles and interacts with the transmembrane spike glycoprotein G. J. Virol. **73:**242–250.
22. **Mitnaul, L. J., M. R. Castrucci, K. G. Murti, and Y. Kawaoka.** 1996. The cytoplasmic tail of influenza virus neuraminidase (NA) affects NA incorporation into virions, virion morphology, and virulence in mice but is not essential for virus replication. J. Virol. **70:**873–879.
23. **Moss, B.** 1995. *Poxviridae*: the viruses and their replication, p. 2637–2672. *In* B. N. Fields, D. M. Knipe, and P. M. Howley (ed.), Fields virology. Lippincott-Raven Publishers, Philadelphia, Pa.
24. **Neumann, G., T. Watanabe, and Y. Kawaoka.** 2000. Plasmid-driven formation of influenza virus-like particle. J. Virol. **74:**547–551.
25. **Niwa, H., Yamamura, K., and J. Miyazaki.** 1991. Efficient selection for high-expression transfectants with a novel eukaryotic vector. Gene **108:**193–199.
26. **Pattnaik, A. K., and G. W. Wertz.** 1991. Cells that express all five proteins of vesicular stomatitis virus from cloned cDNAs support replication, assembly, and budding of defective interfering particles. Proc. Natl. Acad. Sci. USA **88:**1379–1383.
27. **Peters, C. J., A. Sanchez, P. E. Rollin, T. G. Ksiazek, and F. A. Murphy.** 1995. *Filoviridae*: Marburg and Ebola viruses p. 1161–1176. *In* B. N. Fields, D. M.

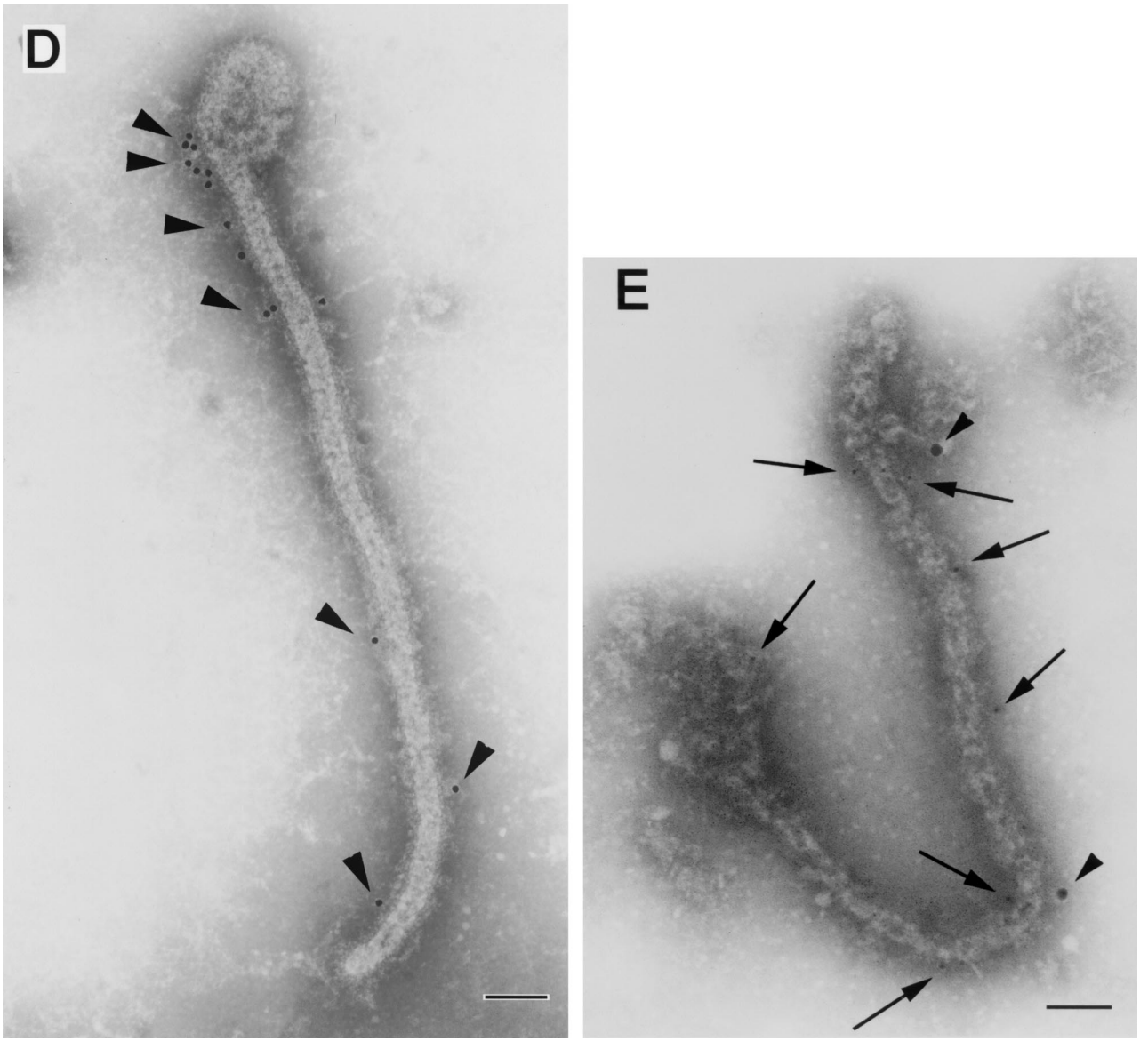

FIG. 6—*Continued*.

Knipe, and P. M. Howley (ed.), Fields virology. Lippincott-Raven Publishers, Philadelphia, Pa.

28. **Robison, C. S., and M. A. Whitt.** 2000. The membrane-proximal stem region of vesicular stomatitis virus G protein confers efficient virus assembly. J. Virol. **74:**2239–2246.
29. **Sakaguchi, T., T. Uchiyama, Y. Fujii, K. Kiyotani, A. Kato, Y. Nagai, A. Kawai, and T. Yoshida.** 1999. Double-layered membrane vesicles released from mammalian cells infected with Sendai virus expressing the matrix protein of vesicular stomatitis virus. Virology **263:**230–243.
30. **Schnell, M. J., L. Buonocore, E. Boritz, H. P. Ghosh, R. Chernish, and J. K. Rose.** 1998. Requirement for a non-specific glycoprotein cytoplasmic domain sequence to drive efficient budding of vesicular stomatitis virus. EMBO J. **17:**1289–1296.
31. **Takada, A., C. Robimson, H. Goto, A. Sanchez, K. G. Murti, M. A. Whitt, and Y. Kawaoka.** 1997. A system for functional analysis of Ebola virus glycoprotein. Proc. Natl. Acad. Sci. USA **94:**14764–14769.
32. **Takada, A., S. Watanabe, K. Okazaki, H. Kida, and Y. Kawaoka.** 2001. Infectivity-enhancing antibodies to Ebola virus glycoprotein. J. Virol. **75:**2324–2330.
33. **Timmins, J., S. Scianimanico, G, Schoehn, and W. Weissenhorn.** 2001. Vesicular release of Ebola virus matrix protein VP40. Virology **283:**1–6.
34. **Tran Van Nhieu, G., E. Caron, A. Hall, and P. J. Sansonetti.** 1999. IpaC induces actin polymerization and filopodia formation during *Shigella* entry into epithelial cells. EMBO J. **18:**3249–3262.
35. **Volchkov, V. E., V. A. Volchkova, W. Slenczka, H.-D. Klenk, and H. Feldmann.** 1998. Release of viral glycoproteins during Ebola virus infection. Virology **245:**110–119.
36. **Zhou, D., M. S. Mooseker, and J. E. Galan.** 1999. An invasion-associated *Salmonella* protein modulates the actin-bundling activity of plastin. Proc. Natl. Acad. Sci. USA **96:**10176–10181.